Bulletin of the Seismological Society of America, Vol. 73, No. 5, pp. 1415–1434, October 1983

PRECURSORY SURFACE DEFORMATION IN GREAT PLATE BOUNDARY EARTHQUAKE SEQUENCES

BY V. C. LI AND J. R. RICE

ABSTRACT

We present an analysis of time-dependent precursory source processes and associated ground surface deformation prior to the great earthquake rupture of a long seismic gap zone along a transform plate boundary. This work is based on a theoretical model proposed by Li and Rice (1983) and reviewed briefly here. In the model, thickness-averaged stress transmission in the lithosphere is analyzed by a generalized Elsasser plane stress model which includes coupling to a viscoelastic asthenosphere. Upward progression of preseismic rupture at each section along strike is analyzed as quasi-static extension, in local antiplane strain, of an elastic-brittle crack; this provides the necessary boundary condition (in the context of the "line-spring procedure") along strike for the Elsasser plate model. The approach to instability is simulated using what are thought to be typical material and tectonic parameters. It is found that prior to a large earthquake, the shear strain increases rapidly near the seismic gap zone but tends to diminish at moderate distances from the plate boundary. Such a strain-reversal phenomenon, although difficult to measure at present due to its small magnitude, may be helpful in the interpretation of geodetic measurements and in the planning of geodetic network locations for the purpose of earthquake prediction. The acceleration of slip, with consequent acceleration of stress increase in the upper brittle crust, predicted by the model may provide a plausible explanation for nonlinear features associated with seismicity preceding some major events (see, e.g., Raleigh *et al.*, 1982). A "precursor time", t_{prec}, during which anomalous strain rate at the seismic gap exceeds twice its background level, is found to be in the range of a couple of months to 5 yr, depending on the tectonic loading rate; t_{prec} varies approximately as $R^{-1.3}$ (where R is a dimensionless loading rate parameter). This precursor time may be associated with physical anomalities related to rapid stress increase such as ground tilting, water table variation, and radon emission which precede some large earthquakes. Consistent with observations, the analysis predicts longer precursor times for larger earthquakes.

INTRODUCTION

It has been observed that the majority of great shallow earthquakes occur at tectonic plate boundaries, and that some have rupture lengths in the hundreds of kilometers, or several times the lithospheric thickness. These earthquakes involve a finite segment of the plate boundary which undergoes sudden stress drop accompanied by relative slip between the broken fault surfaces. In this paper, we are interested in the time-dependent processes preceding seismic rupture at such a plate segment under increasing tectonic load. These processes include the quasi-static progression of zones of slip or concentrated shearing at the soon-to-rupture segment as well as the resulting precursory ground surface deformation.

According to Reid's (1910) theory, tectonic loading causes the accumulation of elastic strain (near a locked segment along a plate boundary) which is released in an earthquake. Superimposed on this strain field is that due to any preseismic fault slippage at depth in the lithosphere. Such slip is plausible because the presence of large-scale, block-like, tectonic movement implies that material deep in the lithosphere at a plate boundary takes on large concentrated shear deformations. Presum-

ably, the high temperature and pressure at depth allow aseismic inelastic shear displacement along deep portions of a plate boundary, consistent with the relative shallowness of the seismogenic layer. The picture emerging is that a crack-like zone of slip or concentrated shear spreads upward from the base of the lithosphere at a plate boundary and progresses toward the surface due to increasing tectonic load (Figure 1, a and b). Such a manner of loading the shallow and apparently brittle

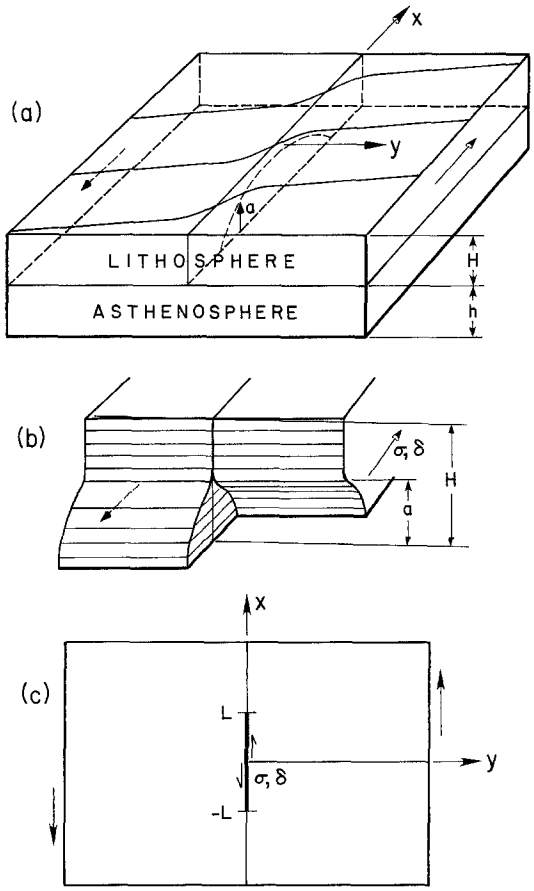

FIG. 1. (a) Coupled lithosphere/asthenosphere system showing zone of slip or concentrated shear deformation progressing upward at a plate boundary. (b) Antiplane strain model of local section at $x =$ constant showing slip zone progression from which the constitutive relation $\sigma = f(\delta)$ is derived. (c) Two-dimensional plate representation of (a); $\sigma - \delta$ relation from (b) holds along discontinuity $-L < x < L$.

portions of the lithosphere has been discussed by many authors (e.g., Savage and Burford, 1973; Turcotte and Spence, 1974; Turcotte *et al.*, 1979; Prescott and Nur, 1981; Dmowska and Li, 1982), and the preinstability slip processes implied have been modeled by Stuart (1979a, b), Stuart and Mavko (1979), and Nur (1981). In this paper, and in a companion paper (Li and Rice, 1983) on which it is based, we emphasize the important role which coupling of the lithosphere to the asthenosphere plays in the preinstability processes; this seems otherwise to have been neglected. We also take into account the finiteness of the rupture length along strike, which has been ignored in much of the existing modeling. We assume that the ends of the slip zone (perhaps representing a "seismic gap zone"), Figure 1a, are bounded by material or geometric barriers, or are a result of the destressing of material outside

the gap by stress drops in recent adjacent ruptures. Results by Li and Rice (1983) for rupture of a transform boundary, expanded upon here and based on their "elastic-brittle crack" model of rupture progression, suggest that upward extension of this slip zone is stable until some time before the earthquake on the order of several months to several years (based on representative values for material and fracture parameters that they infer; see subsequent discussion on "Precursor Time"). It is this final stage of the slip zone progression that we shall address in the present paper. Indeed, although the elastic-brittle model of plate boundary response is hardly adequate for describing the activation of slip at depths of ductile shear flow, it does seem appropriate for this final stage which, as will be seen, involves upward penetration of the slip zone through the strongest portions of the brittle seismogenic layer. We focus, in particular, on the ground surface strain and strain rate during this final period, since a description of their time and space characteristics may form a basis for interpreting possible precursory signals to an imminent great earthquake.

The basic modeling of the upward progression of rupture described above has been carried out in the companion paper. To make this paper self-contained, however, the modeling procedures are first described briefly. But primary emphasis is placed on presentation of results on the time-dependence of the rupture process and associated consequences for surface strain and strain rate.

The Modeling Procedure

The lithosphere/asthenosphere system with a seismic gap zone is modeled as a two-dimensional plate containing a discontinuity along $-L < x < +L$ (Figure 1c). With increasing tectonic loading, the plate is assumed to undergo "generalized" plane stress deformation. In the context of a linear formulation, the lithosphere thickness-averaged shear stress σ ($= \sigma_{xy}$, x directed along strike, y perpendicular) on the discontinuity may be related to arbitrary thickness-averaged slip $\delta(x, t)$ [$\equiv u_x(x, y = 0^+, t) - u_x(x, y = 0^-, t)$], within the approximation of a two-dimensional plate model, by,

$$\sigma(x, t) = \sigma_0(x, t) - \int_{-L}^{L} \int_{-\infty}^{t} g(x - x', t - t') \frac{\partial^2 \delta(x', t')}{\partial x' \partial t'} dt' dx' \qquad (1)$$

where $\sigma_0(x, t)$ is the tectonic stress that would be transmitted across the plate boundary in the absence of slip (see section on "Tectonic Stressing Rate" for detailed discussion of σ_0). Here, $g(x, t)$ is a Green's function which represents the structural stiffness of the earth model. The explicit time-dependence of $g(x, t)$ is appropriate when account is taken of viscoelastic mantle deformation as in our present modeling. In fact, $g(x, t)$ is the thickness-averaged stress at a point x along strike and at time t due to a unit dislocation of thickness-averaged slip suddenly introduced uniformly along $x \leqq 0$ and at time $t = 0$. Of course, this two-dimensional plate model by itself cannot account for details of the slip process along the plate boundary. To supply it with the missing information in the depth-wise direction at the discontinuity, an antiplane strain model (Figure 1b) is adopted to represent slip progression at each plane slice x = constant. Specification of depth-wise variation of material behavior affords a relation between σ and δ at the plate boundary. Thus

$$\sigma(x, t) = f[\delta(x, t), x]. \qquad (2)$$

The explicit x dependence allows the possibility of mechanical heterogeneity along

strike. Equations (1) and (2) combine to form a closed system, from which $\sigma(x, t)$ and $\delta(x, t)$ may be solved, once $\sigma_0(x, t)$ is specified. Such an approach is really a simple generalization of the Rice and Levy (1972) "line-spring" procedure for analyzing part-through tensile cracks in elastic plates. Essentially, it recognizes that owing to the part-through cracked section, the lithospheric plate has severe local concentrations of strain over distances from the fault surface of extent comparable to the plate thickness (Figure 1a). Such concentrated deformations are conveniently lumped into a discontinuity along strike of the plate boundary (Figure 1c). The modeling procedure described is quite general and can take on any degree of sophistication in the description of the lithosphere/asthenosphere system [i.e., $g(x, t)$] and in the description of the mechanical property of the seismic gap zone [i.e., $f(\delta, x)$]. For illustration, a specific earth model and a plate boundary slip-progression model is presented in the following two sections. There, two simplications are adopted. First we ignore nonuniformity of mechanical strength along strike so that $\sigma(x, t) = f[\delta(x, t)]$ only. Second, we treat σ and δ as uniform along a long seismic gap zone ($2L > H$), as in the "single degree of freedom" procedure of Li and Rice (1983). Thus, equation (1) may be replaced by a relation between $\sigma(t)$, $\sigma_0(t)$, and $\delta(t)$, conveniently written in an inverted form as

$$\delta(t) = \int_{-\infty}^{t} C(t - t') \frac{d}{dt'} [\sigma_0(t') - \sigma(t')]dt' \tag{3}$$

where $C(t)$ is a compliance of the adopted earth model. Relaxation of the above simplications have been attempted by Li (1981) only in the case when the asthenosphere is uncoupled from the lithosphere.

Time-dependent compliance of the generalized Elsasser model. The plate model adopted here is the generalized Elsasser model developed by Rice (1980) and discussed in detail by Lehner *et al.* (1981). It treats the lithosphere as an elastic plate (with shear modulus G and Poisson's ratio ν) of thickness H which can undergo elastic plane stress deformations and which rides on a Maxwellian viscoelastic asthenospheric foundation with averaged viscosity η and thickness h (Figure 1a). Consideration of the thickness-averaged stress equilibrium equation, the plane stress-strain relation and an elementary Maxwell model of the foundation (Lehner *et al.*, 1981) leads to the equations governing the in-plane thickness-averaged displacements $u_j(x, y, t)$ (where $j = x, y$)

$$\left(\alpha + \beta \frac{\partial}{\partial t}\right) \sum_{k=x,y} \left(\frac{\partial^2 u_j}{\partial k^2} + \frac{1 + \nu}{1 - \nu} \frac{\partial^2 u_k}{\partial j \partial k}\right) = \frac{\partial u_j}{\partial t}.$$

$$\alpha = hHG/\eta, \qquad \beta = bH \tag{4}$$

Here, $b \approx (\pi/4)^2 H$ is an effective short-time elastic coupling thickness of the viscoelastic foundation (assumed to have shear modulus G as well) which supplies resistive basal shear to the deformations in the lithospheric plate. It has also been shown that for strike-slip motions, where the predominant displacement u is parallel to the strike of the plate boundary, equation (4) may be replaced with little error by the simpler model equation

$$\left(\alpha + \beta \frac{\partial}{\partial t}\right) \left\{(1 + \nu)^2 \frac{\partial^2 u}{\partial x^2} + \frac{\partial^2 u}{\partial y^2}\right\} = \frac{\partial u}{\partial t} \tag{5}$$

(having associated shear stress $\sigma_{xy} = G(\partial u/\partial y)$, the solution of which matches very well that of (4) in several important limits (Lehner *et al.*, 1981). Of particular interest is the ratio $\beta/\alpha = \eta b/Gh$ which defines the relaxation time of the viscoelastic foundation. For numerical illustrations, we have assumed the values $\eta = 2 \times 10^{19}$ Pa-s, $G = 5.5 \times 10^{10}$ Pa, $h = 100$ km, and $H = 75$ km which gives $\beta/\alpha \approx 5$ yr. [The value of η is based on postseismic rebound studies by Thatcher *et al.* (1980); see also Lehner *et al.* (1981) for details.] For detailed development of equations (4) and (5) and the choice of parameters, the interested reader is referred to the paper by Lehner *et al.* and also to the companion paper by Li and Rice (1983).

Physically, the coupled plate model [equation (5)] describes the transmission of stress in the lithospheric plate. The elastic shear strain stored in the plate and the driving of the episodic movement at the plate boundary depends on the tectonic load σ_0. As we shall discuss in more detail later in this paper, this tectonic load must be related in some manner to the large scale tectonic plate movements remote from the plate boundary. However, the structural compliance $C(t)$ of the coupled plate system also determines the manner in which slip occurs at the plate boundary (much like the behavior of a test specimen with a saw-cut loaded by a machine of finite stiffness). This compliance is necessarily time-dependent because of the coupling to the viscoelastic asthenosphere. For example, if a stress drop suddenly occurs along the plate boundary, the instantaneous reaction of the coupled plates is stiff with the foundation behaving as an elastic solid, whereas the long time reaction is more compliant since then, the foundation is completely relaxed and the elastic lithospheric plate may be regarded as effectively uncoupled from the asthenospheric foundation. The time scale of this relaxation process depends on the relaxation parameter β/α, henceforth denoted t_r, but is several times greater because of coupling to the elastic plates (see Appendix).

The coupled plate compliance is also a function of the length $2L$ of the rupturing zone. The longer the length, the more compliant is the coupled plate system. Indeed, if we imagine a constant stress drop uniform along an infinitely long plate boundary, the compliance tends to infinity as the foundation relaxes so that its load carrying capacity diminishes to zero. In contrast, for a finite rupture length, the stress drop could be carried by the unbroken part of the plate boundary so that the compliance tends to a finite limit, even when the foundation is completely relaxed. Derivation of the compliance $C(t)$ that we use in our work has been carried out by Li and Rice (1983) and is based on the solution to equation (5) given by Lehner *et al.* (1981) in their approximate simulation of a finite zone of uniform stress drop along a plate boundary. The result (Li and Rice, 1983, Appendix 2) can be written in the Laplace transform domain as

$$\hat{C}(s) = \frac{2/L}{(1+\nu)G}\frac{1}{s\lambda}\int_0^L [\text{erf}\sqrt{2\lambda l}]^2 dl \tag{6}$$

where $\lambda = 1/(1+\nu)\sqrt{\beta + \alpha/s}$. Inversion of (6) is not readily available in analytic form. Note that a rupture zone length of $2L$ is assumed, and the relaxation time $t_r = \beta/\alpha$ comes in through λ.

A mode III elastic-brittle crack model of antiplane strain deformation at a plate boundary. The generalized Elsasser model described above deals with deformation in the elastic plate in a thickness-averaged sense. In order to treat the rupture progression at the plate boundary, and especially the surface deformation precursory to an imminent earthquake, it is necessary to supply more detailed description in

the thickness direction. To do this, we model the antiplane strain slip by progression of a crack (of current length a; see Figure 1b) which advances under load σ when the stress intensity factor at the crack tip reaches a prescribed level $K_c = K_c(a)$. The length of the crack corresponds to the depth of slip zone penetration.

Such an elastic-brittle model envisions that once the crack tip has passed a given point, the local shear stress τ there falls to a (possibly depth-dependent) residual level. As commented by Li and Rice (1983), one can measure local stress levels from this residual level, since only changes in stress are relevant for description of changes in strain during the earthquake cycle, and hence, choose the thickness-averaged stress σ so that one would have $\sigma = 0$ in a hypothetical state for which the entire plate boundary was ruptured and slipping simultaneously. The elastic-brittle model therefore models slip, once initiated, as taking place at constant local stress. Ductile shear flow at depths below the seismogenic layer is perhaps better modeled by taking τ as a nonlinear function of local slip rate; but for strong nonlinearity, τ varies little with substantial changes in slip rate, and hence slip at constant τ as in the elastic-brittle model may be an acceptable approximation. This seems particularly so in the present case since we are concerned with the preinstability period during which, so our calculations suggest, increases of σ are serving to drive the advancing tip of the slip region upward through the strongest portions of the seismogenic layer, and material response in that layer might plausibly be taken as elastic-brittle.

For the elastic-brittle crack model, the stress necessary to achieve the critical stress intensity factor and the corresponding thickness-averaged slip are [Li and Rice (1983) as developed from Tada *et al.* (1973)]

$$\sigma = \frac{K_c(a)}{\sqrt{2H \tan(\pi a/2H)}} \tag{7a}$$

$$\delta = \frac{4}{\pi}\frac{H}{G}\sigma \ln\left[\frac{1}{\cos(\pi a/2H)}\right]. \tag{7b}$$

Equations (7) are regarded as a constitutive relation [in the form of equation (2), but now expressed parametrically in terms of a and having no x variation] between the plate boundary stress σ and the plate boundary relative slip δ along $-L < x < +L$. The choice of $K_c(a)$ means a specification of the mechanical property (i.e., $K_c^2/2G$ is the critical fracture energy $\mathcal{G}_c$ of elastic crack mechanics) of fault zone material as a function of depth. Motivated by Stuart (1979a, b), we have assumed the fracture energy to have a Gaussian distribution, reflecting the increase of fracture strength with higher normal pressure across the fault surface with depth and decrease of fracture strength with higher temperature at depth. This decrease corresponds to a decrease in the difference between local stress levels required to initiate slip and those to sustain slip. Presumably, the peak of the fracture energy $\mathcal{G}_{\max} \equiv K_m^2/2G$ occurs at typical focal depths $(H - a_1)$, and the width of the brittle layer is controlled by b (Figure 2). The fracture energy variation thus prescribed confines seismicity in the upper brittle crust, while aseismic yielding occurs below this seismogenic layer.

The elastic-brittle crack model can be regarded as a limiting case of the slip weakening model used by Stuart (1979a, b). Li and Rice (1983) discuss conditions for validity of this limiting case. They also show that instability predictions based

on the elastic-brittle crack model sensibly simulate hypocentral depths, seismic slips, and stress drops in great earthquakes if $H - a_1$, the depth to peak resistance, is taken in the range of 5 to 15 km, b in the range of 5 to 10 km, and $\mathcal{G}_{max}$ around $4 \times 10^6\ J/m^2$ or perhaps a little lower.

The specific simulations that we show in this paper are based on choosing $H = 75$ km, $H - a_1 = 7.5$ km, $b = 5$ km, $\nu = 0.25$, and $\mathcal{G}_{max} = 4 \times 10^6\ J/m^2$. (See the Appendix for the dimensionless form used for the governing time evolution equation.) The results shown are representative of those for other parameter choices in the range cited, and Li and Rice (1983) show how predictions of the model depend on these parameters. Further, although a Gaussian mathematical form is chosen for the distribution of $\mathcal{G}_c$ with depth, Li and Rice comment that only the portion corresponding to values of a in the rise to peak fracture resistance, i.e., a values

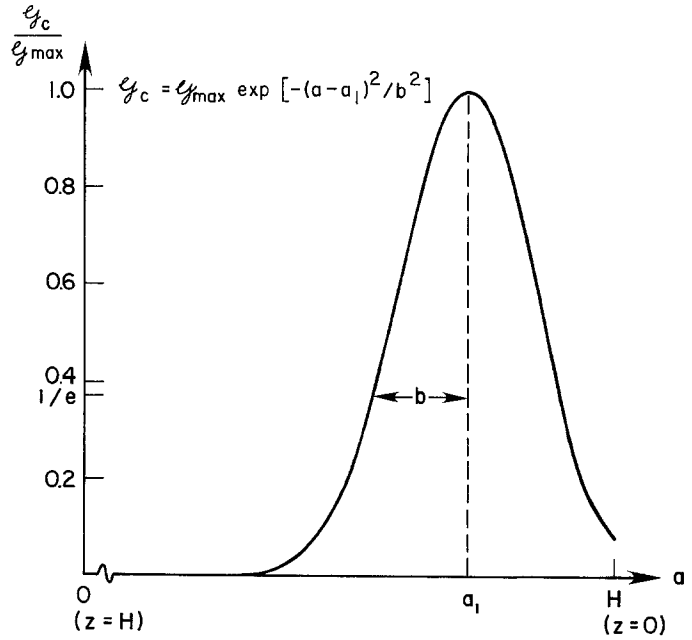

FIG. 2. Fracture energy variation as a function of depth; a is measured from base of lithosphere, $a = H$ is at ground surface, and $a = a_1$ is at maximum fracture resistance. Parameters chosen: $H - a_1 = 7.5$ km; $b = 5$ km.

slightly smaller than a_1, are relevant to the prediction of postpeak (on a σ versus δ plot) behavior and instability.

TIME-DEPENDENT PROCESS AT PLATE BOUNDARY

Equations (2), in the form given by (7), and (3) can be solved numerically (Appendix) to trace the time history of the slip zone progression, if we define that $\sigma = \delta = 0$ at the beginning of the earthquake cycle (σ as well as σ_0 can be measured relative to the residual frictional strength at the completion of the previous earthquake cycle). The σ versus δ relation resulting from the antiplane strain model in equation (7) exhibits deformation weakening behavior. This means that the plate boundary stress and slip first increase in response to increase in tectonic load σ_0 but, after some slip δ_p to peak strength, σ decreases while δ continues to increase

(Figure 3). This behavior reflects the diminishing load carrying capacity of the plate boundary and naturally leads to instability, or an earthquake.

A period of interest for generation of rapid preseismic time-dependent effects is that between initial instability [corresponding to a state denoted by "I", when the plate boundary following $\sigma - \delta$ relation unloads faster than the relaxed coupled plate system with compliance $C(\infty)$ in response to plate boundary slip] and final, dynamic instability [state denoted by "D", when the plate boundary unloads faster than the unrelaxed coupled plate system with smaller compliance $C(0)$]. During this period, the plate boundary is in a self-driven state, i.e., slip will continue to increase even if the tectonic load is held fixed. These three stages at peak stress "P", initial instability, and dynamic instability are indicated in Figure 3, for a plate segment with rupture length equal to five times the lithospheric thickness.

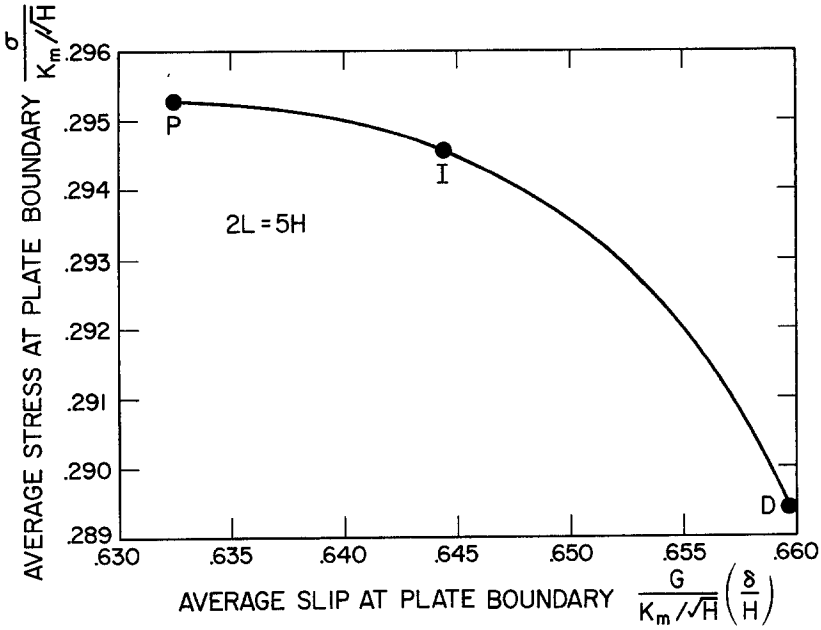

FIG. 3. Postpeak stress-slip relation at plate boundary. The two states of initial instability (I) and dynamic instability (D) are shown for a rupture length equal to five times the lithospheric thickness; (P) denotes peak stress state.

The rapid postpeak stress decrease with time at the plate boundary is shown in Figure 4 for two tectonic loading rates. [The normalizing factor for stress is $K_m/\sqrt{H} \simeq 24$ bars, for $\mathcal{G}_{max} = 4 \times 10^6$ Jm^{-2} and $H = 75$ km; a loading rate parameter R is defined by $R \equiv t_r \dot{\sigma}_0/(K_m/\sqrt{H})$.] It must be kept in mind that this is a thickness-averaged stress, so that the stress level in the upper locked crust will actually be increasing since a higher level of stress is being transmitted across a smaller surface area. An estimate of this smaller area may be obtained by considering the amount of slip zone penetration a into the lithosphere which is shown in Figure 5. The unslipped portion is proportional to $(H - a)$, which decreases with time. Figure 5 is drawn in such a way that the normalized penetration depth increases from zero to one in the growth from peak stress P to dynamic instability D. Figure 6 shows the normalized thickness-averaged slip δ, which, like the slip zone penetration a, accelerates as dynamic instability approaches. The rapid increase of slip coupled with the fact that the slip front is penetrating the brittle (high-fracture energy)

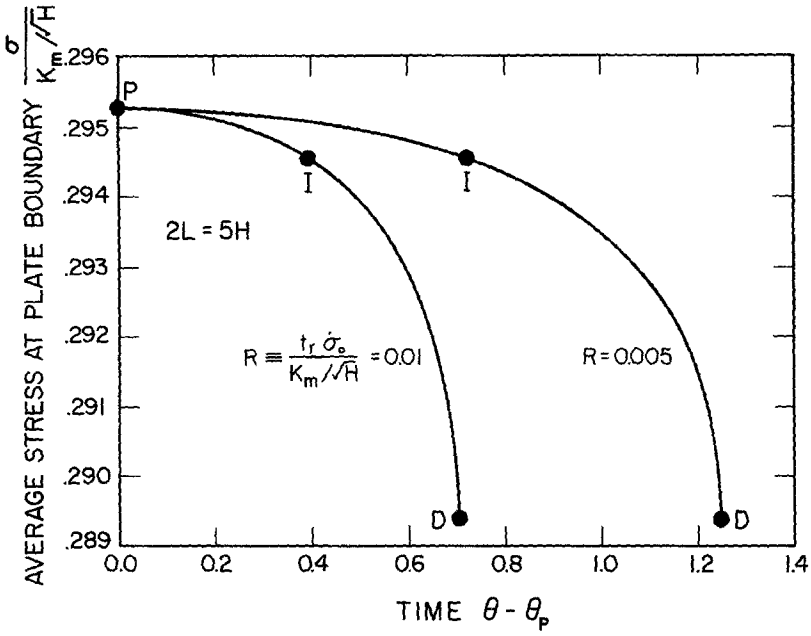

FIG. 4. Thickness-averaged stress decrease with time toward dynamic failure, for two tectonic stress rates and for rupture length equal to five times the lithospheric thickness; $\theta = t/t_r$ is time normalized with respect to asthenosphere relaxation time $t_r \equiv \beta/\alpha$.

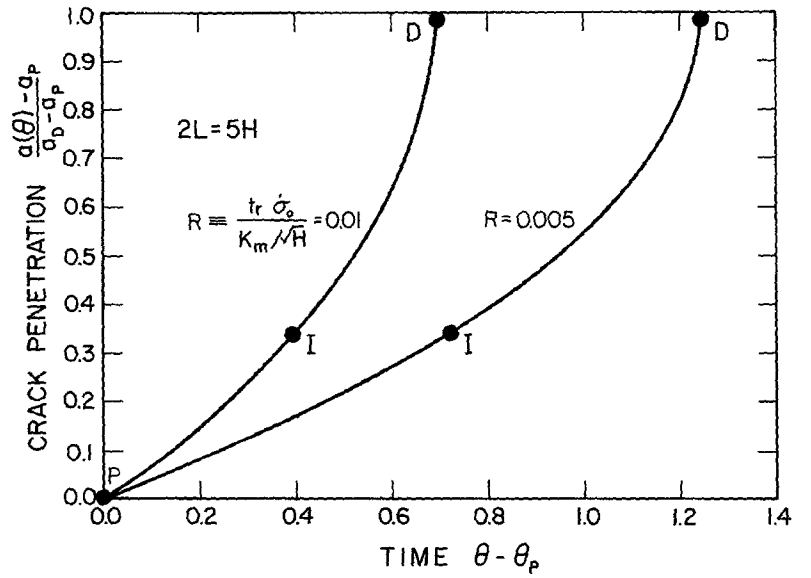

FIG. 5. Normalized crack (slip front) penetration accelerates with time toward dynamic failure; shown for two tectonic stress rates and for rupture length equal to five times the lithospheric thickness. For parameters chosen, $H - a_P = 8.63$ km, $H - a_D = 7.68$ km.

crust suggest the possibility of short-term increased seismicity prior to a large earthquake. Indeed, Raleigh *et al.* (1982) observe that "the strains that ultimately lead to [great plate boundary] earthquakes accumulate non-linearly" and that periods of high-regional seismic activity are often associated with large or major

earthquakes. It should be clear from Figures 5 and 6 that da/dt and $d\delta/dt$ approach infinity as instability is reached, which is characteristic of most quasi-static instability models (Stuart, 1979a, b). As shown in Figures 4 to 6, the change of a, δ, and σ with respect to time depends on the tectonic loading rate $\dot{\sigma}_0$, for a given rupture length. Dynamic instability arrives earlier for a higher $\dot{\sigma}_0$.

Surface Deformation

Although the slip front position and the plate boundary stress and slip are useful in describing the time-dependent preinstability process of rupture progression, it is the surface deformation that is directly measureable by geodetic means and is, therefore, perhaps more important in terms of earthquake prediction. The near-fault surface deformation can be obtained from the antiplane shear crack model shown in Figure 1b. From a modification of the solution for an infinite plate containing collinear cracks under mode III loading [e.g., Tada *et al.* (1973)], the

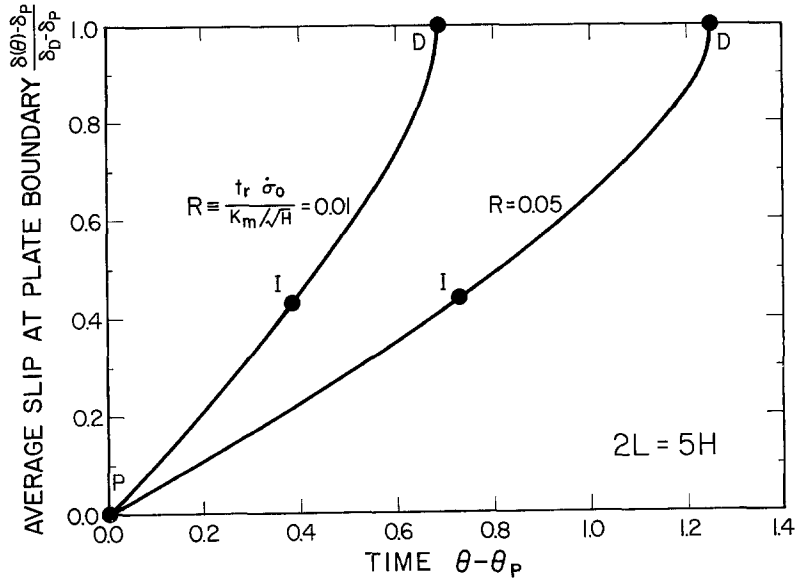

FIG. 6. Normalized slip accelerates with time toward dynamic failure; shown for two tectonic stress rates and for rupture length equal to five times the lithospheric thickness.

surface shear (tensorial) strain at a distance y from the plate boundary is

$$\varepsilon = \frac{\sigma}{2G} \cosh\left(\frac{\pi y}{2H}\right) \left[\sinh^2\left(\frac{\pi y}{2H}\right) + \cos^2\left(\frac{\pi a}{2H}\right)\right]^{-1/2}. \tag{8}$$

The characteristics of near-fault surface deformation are influenced by the following two factors: first, the slip softening behavior causes a decrease in thickness average stress σ, and hence in surface strain at moderately remote distances y, perhaps of the order of a lithospheric thickness from the plate boundary [Stuart (1981) has commented on this in a simpler context]. But, second, the approach of the slip front toward the ground surface along the plate boundary trace causes a local accumulation of strain there, which would be expected to dominate within

distances on the order of the unbroken ligament (i.e., lithospheric thickness H minus the slip zone penetration a) if, as is assumed in this model, precursory slip occurs more or less in a plane. Outside this distance, the softening factor dominates. These two opposing effects create an interesting phenomenon of strain reversal, as shown in Figure 7, a and b, which gives the normalized surface shear strain profile at three different times (at peak stress, at initial instability, and just before dynamic instability) for two rupture lengths. At distances less than $0.2H$ from the plate boundary, the strain increases with time while at distances beyond $0.2H$ the strain

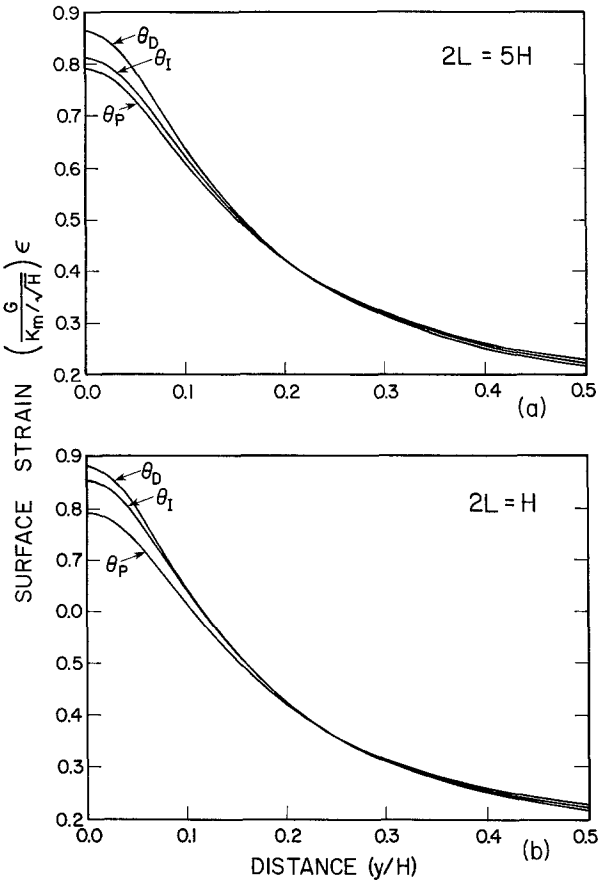

FIG. 7. Surface shear strain profiles for three different times (at P, I, and D) and for rupture lengths (a) five times and (b) equal to the lithospheric thickness. Note strain reversals, slightly exaggerated for clarity.

decreases. Presumably, this distance is related to the depth $H - a_1$ of the fracture energy peak, taken as $0.1H$ here.

The magnitude of the strain changes between peak stress and initial instability, and between initial instability and dynamic instability can be better appreciated in Figure 8, a and b. They show that even though strain softening occurs, the amount of strain reduction [on the order of 0.1 μstrain for $(K_m/\sqrt{H})/G$ chosen as earlier] tends to approach the limit of current geodetic measuring precision (Thatcher, 1981) and may, therefore, not be easily detectable from background noise. The near-fault strain increase, however, should be quite measurable. For example, the strain

increase at the plate boundary ($y = 0$) during the self-driven period ranges from 1.1 μstrain for $2L = H$ to 2.2 μstrain for $2L = 5H$. This is approximately an order of magnitude higher than for a uniform strain accumulation model (i.e., with strains based on changes in σ_0/G).

The surface strain discussed above is defined equal to zero at the beginning of the current earthquake cycle. At times, it may not be easy to establish such a reference level due to lack of geodetic network coverage. It may, therefore, be instructive and useful to consider the strain rate rather than the strain itself. The strain rate is positive and increasing where the slip front advancement factor dominates and is negative and decreasing where the softening factor dominates, as shown in Figure 9, a and b. The shapes of these curves are of course dependent on the tectonic stress rate. What is somewhat surprising here is that the strain rate does not take off rapidly once the self-driven stage arrives but seems to linger on

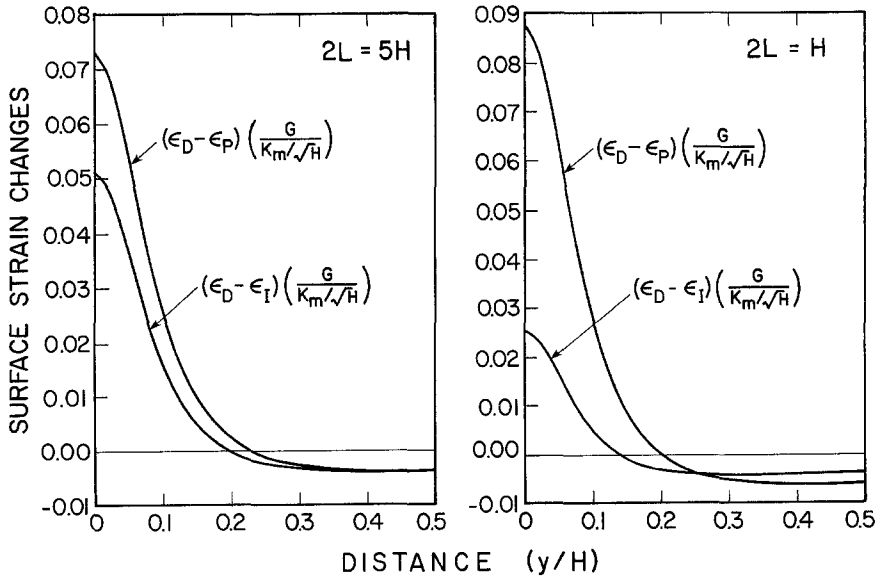

FIG. 8. Surface shear strain changes between P and D and between I and D for rupture lengths (*left*) five times and (*right*) equal to the lithospheric thickness.

until the last quarter of the self-driven period during which the strain rate changes (increase at $y = 0$) rapidly toward dynamic instability. (At this stage, a is close to a_1 where $\mathcal{G}_c$ peaks). The implications of this strain acceleration period before dynamic instability are further discussed in the following section entitled "Precursor Time".

The time-dependent surface deformation discussed so far indicates the general trend of what geodetic measurements might seek in relation to an imminent earthquake. However, there are reasons to expect possibly strong deviations from these results even if our general picture of upwardly progressing slip rupture is correct. For example, the assumption of a lithosphere of homogeneous material is obviously violated; variations in mechanical properties of surface rock are the rule rather than the exception, and this complicates the analysis of surface strain. Another complication may come from slip of nearby or branch faults as mapped, e.g., along the San Andreas fault system. A third factor influencing the surface

strain profile may come from the fact that fault properties or geometry are not homogeneous along strike and so our assumption in this model of a more or less uniform stress distribution would be violated. This last effect may be accounted for by introducing "asperities" into the fault as in Li (1981) and Dmowska and Li (1982), and will be discussed in detail in a separate paper. The results presented here should therefore be regarded only as a general guide to interpreting strain data.

Precursor Time

In the discussion of surface deformation, we show that the near-fault ($y < 0.2H$, or within 15 km of the fault traces for 75-km-thick lithosphere) strain rate increases

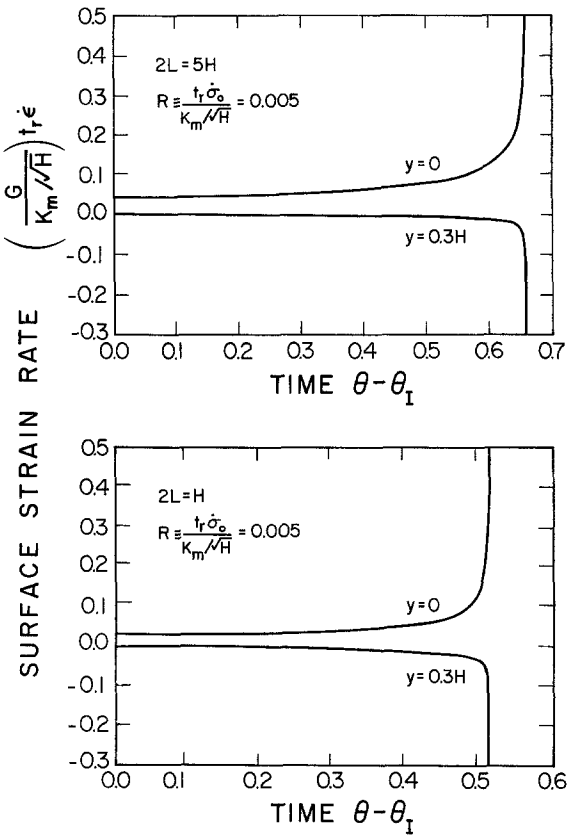

FIG. 9. Surface strain rate change with time at the plate boundary and at $0.3H$ away, for rupture lengths (*top*) five times and (*bottom*) equal to the lithospheric thickness.

rapidly as an earthquake approaches (Figure 9, a and b). It may be expected that this higher strain rate will be accompanied by physical changes in the upper crust, inducing anomalies such as ground tilting. Other precursory phenomenon, such as water table variation, radon emission, etc., may also come into effect because of rock dilatancy caused by the rapid stress increase in the fault vicinity. Thus, for prediction purposes, it should be useful to have an estimate of the time scale when such precursory anomalies may be expected to occur according to our model.

To quantify this time scale, we define (necessarily, somewhat arbitrarily) a precursor time t_{prec} here as the period between t_A and t_D, where t_A is the time when the near-fault strain rate has doubled that at initial instability t_I, and t_D is the time

of dynamic instability. In other words, the strain rate in the precursory period has value at least double that of the background level near the plate boundary, while the strain rate may noticeably decrease further away (e.g., at $y \simeq 0.3H$, Figure 9, a and b). It is found that such a precursor time increases with rupture length but decreases with tectonic loading rate (Figure 10), approximately with t_{prec} proportional to $R^{-1.3}$. The former relation between precursor time and rupture length has been suggested by several studies of observed anomalies prior to large earthquakes (e.g., Rikitake, 1976; Scholz *et al.*, 1973). The relation between precursor time and stressing rate, although intuitively appealing, has not been carefully studied. It

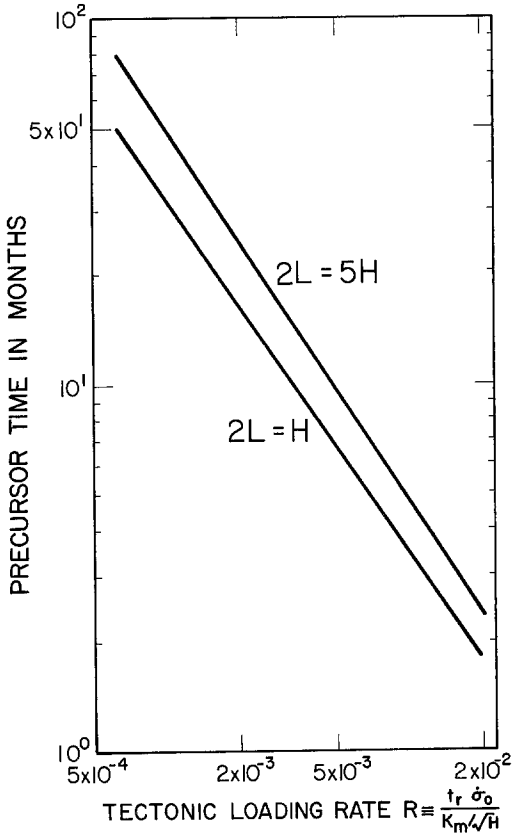

FIG. 10. Precursor time as a function of tectonic loading rate for two rupture lengths. See text for definition of precursor time.

implies that a seismic gap in a plate with high velocity (or high convergence rate at a subducting plate boundary) should have a shorter precursor time, other parameters being equal. For constant tectonic stressing rate of 0.006 to 0.1 bar/yr (which should cover most situations, see discussion in the next section), we find the precursor time to be in the range of a couple of months to 5 yr, which falls within the precursor times suggested by studies of Rikitake and Scholz *et al.* The present calculation is based on $H = 75$ km, $H - a_1 = 7.5$ km, and $b = 5$ km. For a broader brittle zone b or deeper fracture peak $H - a_1$, it is found that both initial and dynamic instabilities occur earlier [i.e., at smaller a_I and a_D, Li and Rice (1983)]. It also appears that the surface strain rate proceeds to accelerate at a time closer to dynamic instability,

resulting in a shorter precursor time. This reflects the deeper source of stress concentration ($H - a_D$) and hence lesser effect on precursory deformation near ground surface.

It should be noted that the results obtained from this crude model must be taken as valid in an order of magnitude sense only. Indeed, mechanisms other than asthenospheric coupling may also be responsible for some of the precursory anomalies (e.g., fluid flow in dilating rocks, rate dependence of slip rupture, etc.).

Tectonic Stressing Rate

The results presented in the previous sections depend on the tectonic loading rate $\dot{\sigma}_0$, which has been assumed to be constant during the time period of interest in our calculations. In this section, we shall try to justify this assumption and the range of $\dot{\sigma}_0$ that we have used in our numerical illustrations, particularly for the estimation of precursor times (previous section and Figure 10). The "tectonic stress" σ_0 has the precise interpretation as the stress that would have been transmitted across the plate boundary segment had there been no slip since the beginning of the current earthquake cycle. Preseismic slip (appearing in our model as a nonzero thickness-averaged δ due to slip at depth associated with advancement of the slip front) diminishes this stress by an amount equal to the integral term in equation (1). Physically, the tectonic stress accumulation is related to (more or less uniform) plate movements far from the plate boundary on the order of a few centimeters per year. The tectonic stress rate varies over the period of a earthquake cycle. Immediately following the previous earthquake in the plate segment of interest, the high stresses thereby shed to depths below the seismic rupture zone cause relaxation processes in the upper mantle to transfer stress onto the lithospheric plate boundary at a fast rate. This rate (and thus the tectonic stress rate on the lithospheric plate boundary) decreases over the relaxation time of the time-dependent process in the upper mantle. The stress transfer process has been studied by Lehner and Li (1982) in the context of the same generalized Elsasser plate model as is used here. They analyzed the lithospheric thickness-averaged strain rate associated with the relaxation process of a viscoelastic asthenosphere in an earthquake limit cycle. Their results indicate that the strain rate decreases significantly at the plate boundary segment over the entire period when the cycle is short (40 yr). However, it becomes relatively constant after roughly half a cycle when the cycles are moderately long (150 yr), based on a relaxation time of 5 yr for the viscoelastic asthenosphere.

Since the large earthquakes normally have cycles more than a hundred years, it may be safe to assume a uniform value for $\dot{\sigma}_0$ for our purpose, as we are interested in a relatively short time period (typically less than one-tenth of repeat time) before an imminent earthquake. Assuming a lithospheric thickness of 75 km and plate velocity of 3 cm/yr, the analysis of Lehner and Li (1982) gives a thickness-averaged stress rate of 0.02 bar/yr near the end of 150-yr earthquake cycle.

Adopting a different point of view, if typical interplate earthquakes have a stress drop of, say 30 bars (Kanamori and Anderson, 1975) and if the dynamic rupture occurs over a 15-km brittle layer in a 75-km thick lithosphere, then the thickness-averaged stress drop would be 6 bars. If this stress drop is a result of stress accumulation at a constant rate over the same 150-yr cycle, then the average stress rate would be 0.04 bars/yr. This averaged over-the-cycle stress rate may be treated as an "upper bound", while the end-of-cycle stress rate from the analysis of Lehner and Li may perhaps be regarded as a reasonable "lower bound".

If we extend the above argument to a typical range of cycle times from 100 to 300 yr, the corresponding "upper bound" range of stress rate would be 0.06 to 0.02 bar/yr while the "lower bound" range of stress rate could be 0.03 to 0.006 bar/yr. Actually, the real stress rate may be even higher than what we have just estimated as an "upper bound". This is because recent adjacent ruptures may transfer stress onto the plate boundary segment of interest. Such a stress diffusion process along strike has been discussed in detail by Lehner *et al.* (1981) in connection with the study of migration of large earthquakes along a plate boundary. They show that a great earthquake rupture can raise the stress rate at a nearby location on the order of 50-km distance along strike by as much as $1\frac{1}{2}$ times, although exact values of this factor depend on cycle time, rupture length, stress drop, and distance of point of interest to previous earthquake location (for more details, see Figure 8 and discussion of Lehner *et al.*, 1981). Thus to include all possibilities, it would perhaps be suitable to adopt a stress rate $\dot{\sigma}_0$ ranging from 0.006 to 0.1 bar/yr, for the purposes of analyzing the time-dependent postpeak (referring to the slip softening $\sigma - \delta$ behavior) source rupture process. It is expected that errors would not be significant even if a constant stress rate is used starting at a state before peak, as long as the time period from this state to dynamic instability constitutes less than half the cycle time. The corresponding range of the dimensionless rate R, choosing other parameters as earlier, is approximately 0.001 to 0.02, and this explains the choices in Figures 4 to 6.

Concluding Discussions

We have presented a method of describing the time-dependent process of preseismic rupture progression at a strike-slip plate boundary and its associated ground surface deformation based on a "line-spring" procedure employing a generalized Elsasser earth model and an antiplane strain shear crack model. We have emphasized the time scale and spatial distribution of precursory strain changes in the hope of improving the current understanding of strain-related phenomena precursory to some large earthquakes.

A basic assumption here is that the plate boundary is a narrow zone where slip displacement can be accommodated by aseismic slip at depth and that the slip deficient upper crust catches up by seismic slip. Advancement of the slip front is represented by a crack-like propagation. It is likely that some kind of healing process may operated under conditions at depth and that there is sensitivity to slip rate in the fracture resistance. Such processes can, in principle, be included in the modeling procedure of Li and Rice (1983), and this is a reasonable aim for further work. However, it is expected that qualitative trends of surface deformation as presented here would not be much affected by including rehealing and other rate effects.

We made no attempt to address the behavior of the seismic gap zone for a complete earthquake cycle, and it is not clear that this can be done sensibly on the basis of the elastic-brittle model. Rather, our attention has been directed here to the final period, typically less than 5 yr duration, of the cycle, just before a large earthquake.

The nonlinear acceleration of surface strain predicted during the later stages of this period is due to the progressive penetration of the slip zone into the brittle seismogenic layer, while lower portions of the shear zone experience constant local stressing, as required by the crack model. For example, the distinctly nonlinear stage of strain build-up for $2L = 5H$ is seen in Figure 9 to start at $\theta - \theta_I = 0.5$.

Calculating a at that time from Figure 5, for $R = 0.005$, and using other parameters as given previously, the depth of the advancing slip zone tip at the onset of the strongly nonlinear strain accumulation is $H - a = 7.8$ km. In this calculation, the brittle zone has its peak fracture strength at 7.5-km depth, and the strength decays over an additional 5-km depth (Figure 2). In fact, as remarked in the caption to Figure 5, for the parameters chosen there peak strength is reached when the advancing tip of the slip zone is at 8.6-km depth, and the final earthquake instability occurs when it has moved upwards to 7.7-km depth. Thus the nonlinear surface strain increases that we show are a direct result of slip penetration through the strongest portion of the seismogenic layer as the gap approaches instability.

The model described in this paper stands in contrast to many earlier fault models in which the earthquake is represented as a suddenly imposed dislocation or array of dislocations on the plate boundary. Here, the earthquake (a slip instability) is achieved more realistically as a result of tectonic loading associated with large scale movements of the lithospheric plate. Only by doing so could precursory crustal deformation be analyzed.

Also, although the model is crude in many ways, it has improved over previous fault models by including the effect of lithospheric coupling to an inelastic (viscoelastic) asthenosphere. We have established that this viscoelastic behavior acts to stabilize the fault from immediate catastrophic failure, giving rise instead to the self-driven creep regime. The slip zone is seen to accelerate, penetrating the brittle upper crust accompanied by increasing average slip while the average stress drops from a peak value, thus contributing to the phenomenon of a small strain reversal at moderate distances from the fault trace. This means that surface shear strain increases rapidly close to the fault trace but decreases (less markedly) further away, as the earthquake approaches. If geodetic measuring precision continues to improve, it may be possible to detect such a strain reversal phenomenon; it could sensibly be taken as a first signal that the plate boundary is approaching instability. A clearer signal may be the strain rate close to the fault trace. It is shown that the strain rate may increase by a factor of two or more over its background level within a precursory time period of a couple of months to several years. Unfortunately, possible sources of contamination of these useful signals are plentiful, such as material inhomogeneity, nearby fault movements and stress heterogeneity along strike.

The precursor time, although somewhat arbitrarily defined, appears to fit in well with the time scales reported as those of precursory phenomenon. Data from Scholz *et al.* (1973) suggest long precursor times (>3 yr) for large earthquakes and hence favor the lower end of the range of tectonic stress rate (<0.005 bars/yr) used in this paper. However, such interpretation must be guarded because the data points used in Scholz *et al.* are for earthquakes with short rupture lengths (<100 km) only, while our analysis procedure is sensible only for rupture lengths at least the thickness of the lithosphere. It is also possible that some physical anomalies (such as change in V_p/V_s) may be related to the rupture progression process at depth and hence occur at an earlier time than anomalies associated with surface deformations. If this is true, then perhaps a longer time period, like that between initial and dynamic instabilities, may be appropriate for defining a precursor time.

In a tectonically different environment (such as a shallow dipping thrust zone), the softening effect may be more prominent than we have suggested here and hence more significance should perhaps be attached to the stress state P. Precursory strain softening has been proposed by Wyss *et al.* (1981), although the observed magnitude appears too high to be accountable by the present model.

For more realistic modeling of plate boundaries, the assumption of uniform stress must be relaxed to allow for the inclusion of strength asperities along strike. This could be done by developing an appropriate $\sigma - \delta$ relation that is position dependent as indicated by the explicit x dependence in equation (2), in which case equation (1) will be solved rather than the simplified equation (3). This has been carried out in a preliminary study by Li (1981) in connection with an attempt to rationalize certain precursory seismicity patterns (Dmowska and Li, 1981). In the preliminary study, however, the asthenosphere was assumed to be fully uncoupled from the lithosphere.

Finally, the "line-spring" procedure adopted in this paper can, in principle, be extended to the study of converging plate boundary earthquakes, even though the present effort has only addressed strike-slip or transform boundary earthquakes. It is expected, despite differences in detail, that the process of strain accumulation and precursory strain changes at a converging plate boundary may share some of the characteristic features described in this paper.

ACKNOWLEDGMENT

The work was supported by NSF and USGS. We have had useful discussions on the work with Renata Dmowska. One of the authors (Li) also thanks M. Ando, T. Haberman, C. Kisslinger, L. Slater, and M. Wyss for helpful and stimulating discussions while he was a Visiting Research Associate during the summer of 1982 at CIRES; he has also benefited from conversations with K. Aki.

The authors would like to thank an anonymous reviewer for valuable comments.

REFERENCES

Dmowska, R. and V. C. Li (1982). A mechanical model of precursory source processes for some earthquakes, *Geophys. Res. Letters* **9,** 393–396.

Kanamori, H. and D. L. Anderson (1975). Theoretical basis of some empirical relations in seismology, *Bull. Seism. Soc. Am.* **65,** 1073–1095.

Lehner, F. K. and V. C. Li (1982). Large-scale characteristics of plate boundary deformations related to postseismic readjustment of a thin asthenosphere, *Geophys. J. Royal Astro. Soc.* **71,** 775–792.

Lehner, F. K., V. C. Li, and J. R. Rice (1981). Stress diffusion along rupturing plate boundaries, *J. Geophys. Res.* **86,** 6155–6169

Li, V. C. (1981). Stressing processes associated with great crustal earthquakes at plate boundaries, *Ph.D. Thesis,* Brown University.

Li, V. C. and J. R. Rice (1983). Pre-seismic rupture progression and great earthquake instabilities at plate boundaries, *J. Geophys. Res.* **88,** 4231–4246.

Nur, A. (1981). Rupture mechanics of plate boundaries, in *Earthquake Prediction, An International Review,* D. W. Simpson and P. G. Richards, Editors, Am. Geophys. Union, Washington, D.C., 629–634.

Prescott, W. H. and A. Nur (1981). The accommodation of relative motion at depth on the San Andreas fault system, *J. Geophys. Res.* **86,** 999.

Raleigh, C. B., K. Sieh, L. B. Sykes, and D. L. Anderson (1982). Forecasting southern California earthquakes, *Science* **217,** 1097–1104.

Reid, H. F. (1910). Permanent displacement of the ground, in *The California Earthquake on April 18, 1906: Report of the State Earthquake Investigation Commission,* Carnegie Institution, Washington, D.C., **2,** 16–28.

Rice, J. R. (1980). The mechanics of earthquake rupture, in *Physics of the Earth's Interior,* A. M. Dziewonski and E. Boschi, Editors, Italian Physical Society/North-Holland, Amsterdam, 555–649.

Rice, J. R. and N. Levy (1972). The part through surface crack in an elastic plate, *Trans. ASME, J. Applied Mechanics* **39,** 185–194.

Rikitake, T. (1976). *Earthquake Prediction,* Elsevier, Amsterdam.

Savage, J. C. and R. O. Burford (1973). Geodetic determination of relative plate motion in central California, *J. Geophys. Res* **78,** 832.

Scholz, C. H., L. Sykes, and Y. Aggarwal (1973). Earthquake prediction: a physical basis, *Science* **181,** 4102.

Stuart, W. D. (1979a). Strain softening prior to two dimensional strike slip earthquakes, *J. Geophys. Res* **84,** 1063.

Stuart, W. D. (1979b). Strain-softening instability model for the San Fernando earthquake, *Science* **203,** 907–910.

Stuart, W. D. (1981). Stiffness method for anticipating earthquakes, *Bull. Seism. Soc. Am.* **71,** 363–370.

Stuart, W. D. and G. M. Mavko (1979). Earthquake instability on a strike slip fault, *J. Geophys. Res.* **84,** 2153.

Tada, H., P. C. Paris, and G. R. Irwin (1973). *The Stress Analysis of Cracks Handbook*, Del Research Corp., Hellertown, Pennsylvania.

Thatcher, W. (1981). Crustal deformation studies and earthquake prediction research, in *Earthquake Prediction: An International Review*, by D. W. Simpson and P. G. Richards, Editors, Am. Geophys. Union, Washington, D.C., 394–410.

Thatcher, W., T. Matsuda, T. Kato, and J. B. Rundle (1980). Lithospheric loading by the 1896 Riku-u earthquake, Northern Japan; implications for plate flexure and asthenosphere rheology, *J. Geophys. Res.* **85,** 6429–6439.

Turcotte, D. L. and D. A. Spence (1974). An analysis of strain accumulation on a strike-slip fault, *J. Geophys. Res.* **79,** 4407–4412.

Turcotte, D. L., R. I. Clancy, D. A. Spence, and F. H. Kuthari (1979). Mechanisms for the accumulations and release of stress drop in the San Andreas fault, *J. Geophys. Res.* **84,** 2273–2282.

Wyss, M., F. W. Klein, and A. C. Johnson (1981). Precursors to the Kalapana $M = 7.2$ earthquake, *J. Geophys. Res.* **86,** 3881–3900.

DEPARTMENT OF CIVIL ENGINEERING
MASSACHUSETTS INSTITUTE OF TECHNOLOGY
CAMBRIDGE, MASSACHUSETTS 02139 (V.C.L.)

DIVISION OF APPLIED SCIENCES
HARVARD UNIVERSITY
CAMBRIDGE, MASSACHUSETTS 02138 (J.R.R.)

Manuscript received 13 October 1982

APPENDIX

Solution method of equation (3). Because of the mathematical complexity of the time-dependent compliance [as given by equation (6)] of the coupled-plate system, a simplification was made by approximating it as the displacement response of a standard linear solid (insert in Figure A1) under a unit step load. Thus, the normalized compliance $[C(\theta) - C(0)]/[C(\infty) - C(0)]$ which runs from 0 in the short time limit to 1 in the long time limit is matched by $1 - e^{-\theta/\gamma}$ (Figure A1). The dimensionless relaxation time constant γ is chosen so that the match is exact when $\theta = \gamma$. This gives $\gamma = 5$ for $2L = H$ and $\gamma = 18.5$ for $2L = 5H$. Even though the approximation is far from perfect, it was found that in a few solutions that were carried out employing both numerical inversion of (6) and the standard linear model, results differed by less than 1 per cent in the cases examined, while economy in computing time justifies the approximation. By differentiating (3) with respect to θ and rearranging, we obtain

$$\frac{d\theta}{d\alpha} = f\left(\alpha, \theta; \gamma, \frac{a_1}{H}, \frac{b}{H}, \frac{2L}{H}, \nu, \frac{t_r \dot{\sigma}_0}{K_m/\sqrt{H}}\right) \tag{A1}$$

where

$$f = \frac{d\delta/d\alpha + C(0)\, d\sigma/d\alpha}{C(0) t_r \dot{\sigma}_0 + C(\infty)\sigma_0/\gamma - (\delta + C(\infty)\sigma)/\gamma}$$

and

$$\alpha \equiv \frac{a}{H}.$$

The parameters a_1, b, and K_m describe the fracture strength of the fault zone (Figure

2), and are discussed in more detail in Li and Rice (1983). Numerical illustrations in this paper are based on $a_1 = 0.9H$, $b = 0.07H$, $\nu = 0.25$, and $\mathcal{G}_{max} = K_m^2/2G = 4 \times 10^6\ \mathrm{Jm}^{-2}$.

The nonlinear first order differential equation (A1) is solved using the Runge-Kutta method. The initial condition is provided by considering an initial penetration

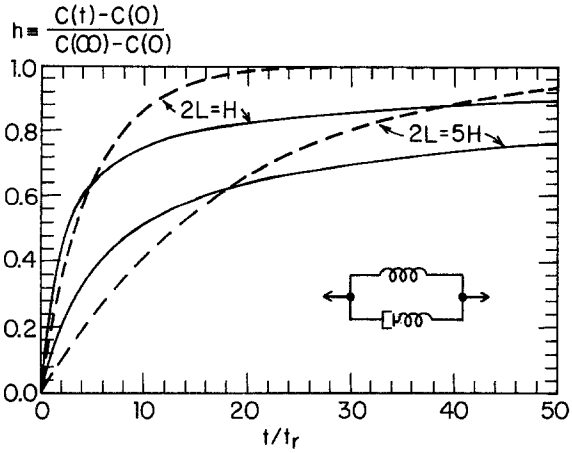

FIG. A1. Approximation of the time-dependent compliance of the coupled-plate system (solid lines) by that of a single parameter standard linear model as shown in dashed lines, for two rupture lengths.

depth a_0 less than that at peak stress. Equation (7) then gives the corresponding σ and δ. If it may be assumed that the plate boundary is in complete equilibrium so that $C = C(\infty)$ (i.e., foundation relaxed), then the corresponding tectonic stress at this initial state is $\sigma_0 = \delta/C(\infty) + \sigma$. Equation (A1) is then solved successively by increments of α for a fixed $\dot{\sigma}_0$, with $\sigma_0 = t_r \dot{\sigma}_0 \theta$.